

# Solvatochromic hydrazone anions derived from chalcones

Daniela Millán, Moisés Domínguez, Marcos Caroli Rezende\*

*Facultad de Química y Biología, Universidad de Santiago, Casilla 40, Correo 33, Santiago, Chile*

Received 17 October 2006; received in revised form 12 July 2007; accepted 22 July 2007

Available online 6 August 2007

## Abstract

The preparation and solvatochromism of anions derived from the 2,4-dinitrophenylhydrazones of 1,3-diphenylpropenone, 1-phenyl-3-(4-nitrophenyl)propenone and 1-phenyl-3-(2-thienyl)propenone are described and their behaviour was interpreted in terms of theoretical calculations of their internal charge-transfer transitions.

© 2007 Elsevier Ltd. All rights reserved.

**Keywords:** Solvatochromic dyes; Hydrazone anions; Chalcones

## 1. Introduction

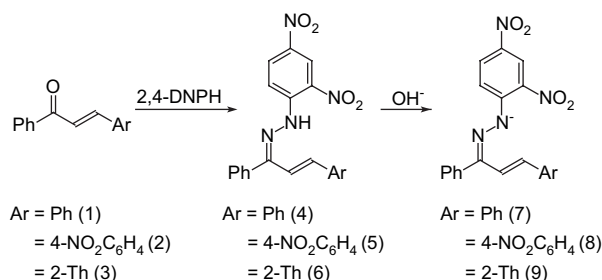
The easy preparation of aryl hydrazones is an attractive feature worth considering in the design of novel solvatochromic compounds which incorporate this fragment in their structure. The hydrazone group may bridge donor and acceptor moieties [1,2] or act itself as a donor fragment, in conjugation with electron-withdrawing groups [3,4]. Tautomeric hydrazone–azo dyes exhibiting a moderate solvatochromic behaviour have also been described [5,6].

Dinitrophenylhydrazones possess an acidic N–H, capable of generating anions with an enhanced electron-donating ability. Conjugation of this nitrogen anion with an acceptor group should lead to potentially interesting solvatochromic dyes.

These considerations led us to investigate the spectral properties of a group of dinitrophenylhydrazone anions. As acceptor groups we employed the 1,3-diarylpropene skeleton of chalcones. Chalcone derivatives have shown interesting properties as optical sensors [7], thanks to their internal charge-transfer absorption in the visible region. Replacement of a phenyl by a thienyl group was expected to enhance the polarizability of the dyes, following reports in the literature

of thienyl derivatives as attractive molecules for the design of nonlinear optical materials [8–11].

In the present report we studied the solvatochromic behaviour of anions **7–9**, easily obtained by treatment with base of the corresponding hydrazones **4–6**, prepared from chalcones **1–3**.



## 2. Experimental

### 2.1. Materials and methods

Melting points were obtained with a Microthermal capillary apparatus and were not corrected. IR spectra were recorded with a Perkin–Elmer 735B equipment, NMR spectra with a 400 MHz Bruker Avance spectrometer, employing tetramethylsilane as

\* Corresponding author.

E-mail address: [mcaroli@lauca.usach.cl](mailto:mcaroli@lauca.usach.cl) (M.C. Rezende).

internal reference. Visible spectra were recorded on a Hewlett–Packard TU-1800 spectrophotometer.

All employed solvents were analytically pure and were employed without any further purification. 1,3-Diphenylpropenone (“chalcone”) (**1**) was prepared by basic condensation of benzaldehyde and phenylethanone [12]. 1-Phenyl-3-(4-nitrophenyl)propenone (“4-nitrochalcone”) (**2**) was prepared by condensation of 4-nitrobenzaldehyde and phenylethanone in boiling water, in the presence of  $\text{Na}_2\text{CO}_3$ , following a reported procedure [13,14].

The 2,4-dinitrophenylhydrazone of the 1,3-diphenylpropenone (**4**) was prepared in 93% yield by treatment of chalcone **1** in methanol with an acidic methanolic solution of 2,4-dinitrophenylhydrazine [14], mp 244–246 °C, lit. [15] mp 248–249 °C. In a similar way, the dinitrophenylhydrazone **5** was obtained in 94% yield from 4-nitrochalcone (**2**) [14], mp 268–270 °C, lit. [16] mp 259–259.5 °C.

**2,4-Dinitrophenylhydrazone of 1-phenyl-3-(2-thienyl)propenone (7)** – to a stirred solution of NaOH (0.5 g, 12.5 mmol) in water (5 mL) and ethanol (3 mL), cooled in a water bath (10–15 °C), was added phenylethanone (1.20 g, 10 mmol) and then 2-thiophenecarboxaldehyde (Aldrich) (1.12 g, 10 mmol). After 4 h, another portion of NaOH (0.4 g, 10 mmol) was added and the mixture was stirred for other 2 h and left standing overnight at room temperature (20 °C) until a solid product separated. The precipitate was filtered and washed with little ice-cold ethanol to give, after drying, 2.04 g (95% yield) of the 1-phenyl-3-(2-thienyl)propenone (**3**), mp 56 °C, sufficiently pure for the subsequent preparation of the corresponding dinitrophenylhydrazone. IR (KBr)  $\nu_{\text{max}}$  1660 (C=O), 1600, 1300 and 1210  $\text{cm}^{-1}$ .  $^1\text{H}$  NMR ( $\text{CDCl}_3$ )  $\delta$  8.00 (2H, d,  $J = 9.6$  Hz, Ar-H *ortho* to C=O); 7.94 (1H, d,  $J = 16$  Hz, CH=CH–CO); 7.59 (1H, m, Ar-H *para* to C=O); 7.50 (2H, m, Ar-H *meta* to C=O); 7.43 (1H, d,  $J = 5.0$  Hz, 3-H of thienyl group); 7.37 (1H, d,  $J = 5.6$  Hz, 5-H of thienyl group); 7.35 (1H, d,  $J = 15.5$  Hz, CH=CH–CO); 7.10 (1H, dd,  $J = 5.0$  Hz,  $J' = 5.5$  Hz, 4-H of thienyl group).

To a hot (90 °C) solution of the prepared propenone (**3**) (1 g, 5 mmol) in ethanol (5 mL) was added an acidified ethanolic solution of 2,4-dinitrophenylhydrazine, prepared by dissolving 1 g (5 mmol) of the hydrazine in ethanol (10 mL) and adding concentrated sulphuric acid (0.5 mL). After cooling, the red precipitate was filtered and dried to give 1.74 g (88% yield) of the 2,4-dinitrophenylhydrazone **6**. The red product was recrystallized from chloroform, mp 239 °C. Analysis, found N 14.56, S 8.33%. Calculated for  $\text{C}_{17}\text{H}_{12}\text{N}_4\text{O}_5$ , N 14.21, S 8.12%. IR (KBr) 3100, 1600, 1500, 1420 and 1320  $\text{cm}^{-1}$ .  $^1\text{H}$  NMR ( $\text{CDCl}_3$ )  $\delta$  11.10 (1H, s, N–H); 9.05 (1H, d,  $J = 2.4$  Hz, H-3 of dinitrophenyl group); 8.34 (1H, dd,  $J = 2.5$ ,  $J' = 9.6$  Hz, H-5 of dinitrophenyl group); 8.11 (1H, d,  $J = 9.6$  Hz, 1H, dd,  $J = 2.5$ ,  $J' = 9.6$  Hz, H-5 of dinitrophenyl group); 7.66 (3H, m, Ar-H); 7.33 (3H, m, Th-H); 7.10 (1H, d,  $J = 16.0$  Hz, Th–CH=C); 7.01 (2H, m, Ar-H); 6.67 (1H, d,  $J = 16.0$  Hz, C=CH–C=N).

The hydrazone anions **7–9** were generated *in situ* by addition of a base to solutions of their conjugate acids. Addition of a KOH pellet to alcoholic solutions of compounds **4–6** was

employed to generate the corresponding anions in protic media. In non-protic solvents, 1–2  $\mu\text{L}$  of a 1 M methanolic solution of tetrabutylammonium hydroxide (Aldrich) sufficed to generate deeply coloured solutions. No attempts were made to estimate the concentration of the generated anions, and consequently of their extinction coefficients, since we were concerned exclusively with the position of the  $\lambda_{\text{max}}$  value of the longest-wavelength band.

Theoretical calculations were performed with the Gaussian 03 package [17] at two levels of theory. At a lower level (method A), the structures of anions **7–9** were optimized with the semi-empirical AM1 method, and the transition energies were then obtained by single-point calculations with the ZINDO/S option [18], employing configuration interactions involving singly excited transitions among the 10 highest occupied and the 10 lowest unoccupied molecular orbitals of the molecules. At a higher level (method B), structures **7–9** were first optimized with a hybrid DFT method (B3LYP//6-31G) [19], and the transition energies were then obtained by performing a TD–DFT calculation (B3LYP//6-31G\*) [20,21].

### 3. Results and discussion

#### 3.1. Solvatochromism of anions **7–9**

Treatment of hydrazones **4–6** with base formed the corresponding anions **7–9** *in situ*. The acidity of compounds **4** and **5** had been measured previously, with  $\text{p}K_{\text{a}}$  values in methanol of 12.3 and 11.2, respectively [14].

The UV–visible spectra of dyes **7–9** were recorded in a variety of protic and non-protic solvents. Table 1 lists the  $\lambda_{\text{max}}$  values of their longest-wavelength bands in various solvents.

Inspection of Table 1 shows that the longest-wavelength  $\lambda_{\text{max}}$  value of dyes **7–9** in the same solvent increased in the order **7** < **9** < **8**. Replacement of a phenyl by the more polarizable thienyl group caused a small bathochromic shift of this

Table 1  
Variation of the  $\lambda_{\text{max}}$  values of the longest-wavelength charge-transfer band of dyes **7–9** in various solvents

Solvent	$E_{\text{T}}(30)$ values, $\text{kcal mol}^{-1}$ [22]	$\lambda_{\text{max}}$ values, nm		
		<b>7</b>	<b>8</b>	<b>9</b>
Methanol	55.4	500	540	510
Ethanol	51.9	506	553	517
<i>n</i> -Propanol	50.7	508	555	516
1-Butanol	49.7	508	556	516
3-Methyl-1-butanol	49.0	512	557	520
2-Propanol	48.4	514	563	524
Dimethylsulfoxide	45.1	541	586	550
Dimethylformamide	43.2	537	583	548
Acetonitrile	45.6	536	582	541
Acetone	42.2	535	590	544
Dichloromethane	40.7	533	590	544
Tetrahydrofuran	37.4	530	605	546
Chlorobenzene	36.8	529	589	540
Ethyl acetate	38.1	529	596	542
Chloroform	39.1	528	586	540

band. This shift was more pronounced when a nitro-substituent was appended to the phenyl group.

For all dyes, distinct solvatochromic trends were observed in protic and non-protic media. In the former, a discernible blue shift resulted from increasing the acidity of the alcoholic solvent. In non-protic solvents  $\lambda_{\max}$  values for a given dye were generally larger than in alcoholic media. For compounds **7** and **9**, a small (*ca.* 10 nm) blue shift of their longest-wavelength  $\lambda_{\max}$  value resulted from decreasing the polarity of the medium. A greater dispersion in the  $\lambda_{\max}$  values was observed for the nitro-derivative **8**, with little consistent variation of the transition energies with the medium polarity. The above observations are graphically illustrated in Fig. 1, where the transition energies of the longest-wavelength bands of compound **7** and of its nitro-substituted analog **8**, expressed as wavenumbers  $\nu_{\max}$ , are plotted against the  $E_T(30)$  values of the employed solvents.

### 3.2. Preferential solvation in a binary mixture

We also carried out a study of preferential solvation for a member of the series, compound **8**, in a binary protic/non-protic mixture of solvents. Fig. 2 depicts the variation of  $\nu_{\max}$  values of this dye in mixtures of DMSO–MeOH of variable composition. The data were fitted to Eq. (1) [23], derived from a simple preferential solvation model that assumes a competitive exchange equilibrium between the two solvent components for the dye solute [24].

$$\nu_{\max} = \nu_{\max}^A + \left( \nu_{\max}^B - \nu_{\max}^A \right) f_{B/A} \cdot x_B / \left[ (1 - x_B) + f_{B/A} \cdot x_B \right] \quad (1)$$

The wavenumber value  $\nu_{\max}$  in a mixture of two solvents A and B is expressed in terms of the molar fraction of B,  $x_B$ , of the wavenumber values of the dye in pure solvents A and B,  $\nu_{\max}^A$  and  $\nu_{\max}^B$ , and of the adjustable parameter  $f_{B/A}$ . The latter, defined as a preferential solvation parameter, measures the tendency of the dye to be solvated by B rather than A. A value

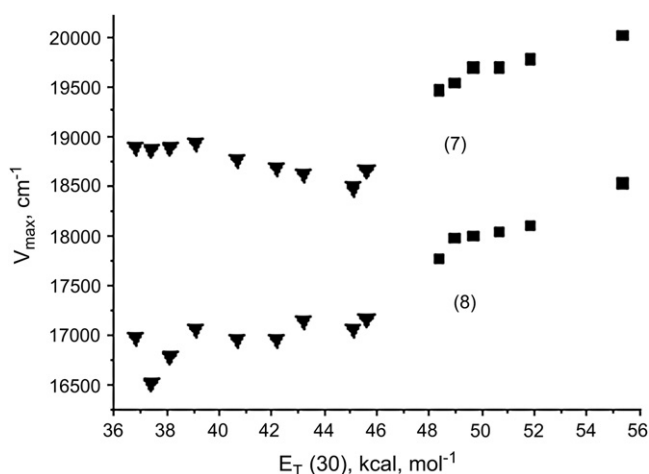


Fig. 1. Variation of the transition energies for the longest-wavelength band of dyes **7** and **8**, expressed in wavenumber values, in solvents of different polarities. Data points refer to protic (■) and non-protic solvents (▲).

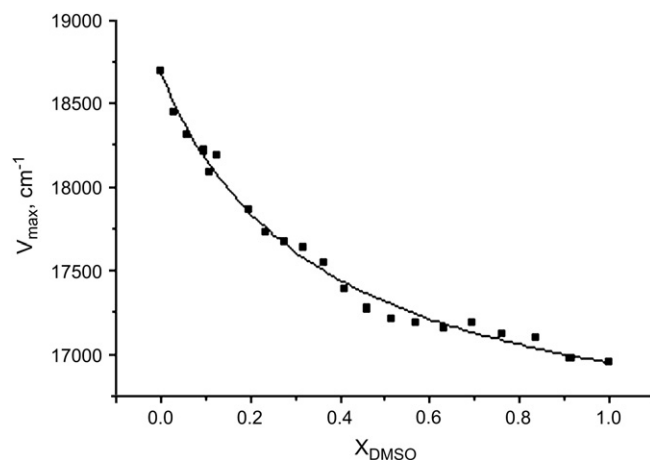


Fig. 2. Variation of the wavenumber value of the longest-wavelength band of dye **8** in mixtures of MeOH–DMSO of variable composition.

of one indicates no preference on the part of the solute. Larger  $f_{B/A}$  values point to an increased preferential solvation by B.

The variation of the  $\nu_{\max}$  values of **8** in MeOH–DMSO mixtures with the increasing molar fraction of the latter solvent is depicted in Fig. 2. The data points were fitted to the curve shown, following Eq. (1), with an  $f_{B/A}$  value of 3.8, in an indication that dye **8** was preferentially solvated by DMSO.

### 3.3. Theoretical calculations

In order to gain a deeper insight into the internal charge-transfer process of the dyes, we performed calculations at two different levels of theory. At a lower level of theory, the structures were optimized with the semi-empirical AM1 method, and the transition energies calculated with the ZINDO/S method. At a higher level of theory, the structures were optimized with the B3LYP//6-31G method [19] and the corresponding transition energies calculated with the TD–DFT option (B3LYP//6-31G\*) [20,21]. Table 2 compares the experimental with the theoretical charge-transfer energies for all cases.

An inspection of Table 2 reveals significant differences between the results of the two methods. The first allowed singlet transition energies of dyes **7–9** were all larger (smaller  $\lambda_{\max}$  values) than the experimental values in chloroform, when the molecules were optimized by the AM1 method and the transition energies calculated with the ZINDO/S and CI interactions. By contrast, the use of DFT methods led to transition energies that were significantly smaller than the experimental ones. The use of a higher level of theory in this case did not lead to any improvement over the semi-empirical AM1–ZINDO/S level. The reason for this may be sought in other reports in the literature, on the limitations of TD–DFT methods for the calculation of transition energies. TD–DFT methods do not perform well with extended  $\pi$  systems, and yield substantial errors for charge-transfer excited states, with drastically underestimated excitation energies [25].

In spite of the opposite trends obtained with the two levels of calculation, the patterns of internal charge-transfer for

Table 2  
Theoretical  $\lambda_{\text{max}}$  values for the longest-wavelength charge-transfer band of dyes **7–9** in the gas phase

Dye	$\lambda_{\text{max}}$ value, nm		
	Experimental <sup>a</sup>	Calculated ( <i>f</i> ) <sup>b</sup>	
		A <sup>c</sup>	B <sup>d</sup>
<b>7</b>	528	510 (1.22)	572 (0.24)
<b>8</b>	585	548 (0.99)	647 (0.37)
<b>9</b>	540	527 (1.19)	585 (0.30)

<sup>a</sup> In chloroform.

<sup>b</sup> Oscillator strengths (*f*) are given in parenthesis.

<sup>c</sup> Method A: AM1 optimization, followed by single-point ZINDO/S calculations employing configuration interactions involving mono-electronic transitions between the 10 highest occupied and the 10 lowest unoccupied molecular orbitals.

<sup>d</sup> Method B: optimization by the B3LYP//6-31G method followed by TD-DFT (B3LYP//6-31G\*) calculations.

compounds **7** and **8** were rather similar, according to the two methods.

The major contributor to the first allowed singlet transition, calculated by the semi-empirical method employing configuration interactions, was found to be in all cases the HOMO–LUMO transition. The TD–DFT calculations also led to the same conclusions. We may then obtain a reasonable picture of the internal charge-transfer transition of these systems by an analysis of these molecular orbitals. Fig. 3 depicts the HOMO and the LUMO of dyes **7** and **8**, calculated by the ZINDO/S method, thus allowing a comparison of the unsubstituted system **7** with its nitro-substituted analog **8**.

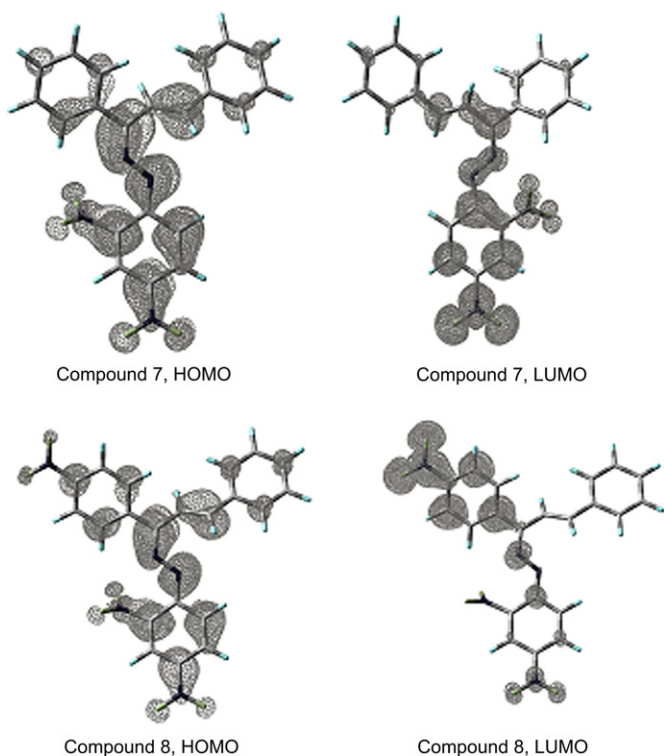


Fig. 3. HOMO and LUMO of dyes **7** and **8**, calculated with the ZINDO/S method.

The theoretical analysis revealed that the solvatochromic behaviour of these systems arises from two different processes, depending on the nature of the acceptor fragment. In both cases, the HOMO density is distributed among the dinitrophenylazo and, to a smaller extent, the phenyl fragments. In the case of the unsubstituted compound **7**, the LUMO distribution concentrates its density on the dinitrophenyl fragment, which is the most electron-withdrawing conjugated ring. A different situation is observed for the nitro-substituted analog **8**. In this case, charge is transferred to the nitro-substituted phenyl ring, as can be seen by its LUMO distribution.

Calculations performed with compound **9** yielded a charge-transfer pattern similar to that of compound **7**, with the LUMO concentrated on the dinitrophenyl fragment. Thus, the solvatochromic band of dyes **7–9** arises from different charge-transfer processes. For the unsubstituted systems **7** and **9**, charge is transferred to the dinitrophenyl fragment, for the nitro-substituted analog **8** to the nitrophenyl group.

### 3.4. Solvent effects on the solvatochromism of **7–9**

The distinct solvatochromic behaviour of all dyes in protic and non-protic media must reflect different solvent effects in these environments. Hydrogen-bond-donor solvents interact with the dyes by partially protonating them in solution. The resulting charge reduction on the nitrogenated donor fragment of these dyes is responsible for the observed blue shift of their  $\lambda_{\text{max}}$  value in increasing acidic alcohols. In non-protic media, however, this effect should be very small or non-existent and we must turn our attention to other contributions to solvation, such as the dipolar character of the solvent. The solvent polarizability seems to be an important factor in the solvation of these anions, as shown by the preferential solvation of **8** by the highly polarizable solvent DMSO, when competing with a strong proton donor like MeOH.

Regression analyses performed on the transition energies of all dyes in the investigated solvents allowed us to estimate the separate contributions of the acidity and the polarizability of the medium to the solvatochromic behaviour of these compounds. This multiparametric approach employed Catalán's SA [26] and SPP<sup>N</sup> [27] parameters for the characterization of the acidity and the polarizability of each solvent. The resulting Eqs. (2)–(4), corresponding to compounds **7–9**, respectively, point to slightly different responses to the two solvent effects on the part of pair **7/9** and the nitro-substituted analog **8**. Opposing contributions of the acidity and polarizability of the medium are observed to the solvatochromism of compounds **7** and **9**. In the case of dye **8**, transition energies increase with the acidity and the dipolarity–polarizability of the solvent (Eq. (3)).

$$\nu_7 = 2393\text{SA} - 2462\text{SPP}^N + 20869 \quad (2)$$

$$N = 15, r = 0.979$$

$$\nu_8 = 2951\text{SA} + 758\text{SPP}^N + 16235 \quad (3)$$

$$N = 15, r = 0.975$$



$$\nu_9 = 2443SA - 1680SPP^N + 19817 \quad (4)$$

$$N = 15, r = 0.971$$

The theoretical analysis of the internal charge-transfer process in these anions may shed light on their spectral behaviour in solution. Replacement of a phenyl by the more polarizable thienyl group led to little change in the solvatochromic behaviour of dyes **7** and **9**. By contrast, the introduction of a nitro-substituent in **8** led to significant changes, with larger bathochromic shifts of its solvatochromic band. This is explained by the different charge-transfer processes that take place for dyes **7** and **8**, as shown in Fig. 3. As discussed above, in all dyes charge is transferred from the same donor fragment, the dinitrophenylazo moiety. Partial protonation of the anionic nitrogen atom of this fragment leads to HOMO stabilization by a protic solvent, and a consequent increase of the HOMO–LUMO transition energy, an effect which is common to all dyes. However, in non-protic media, transition energies are governed by the interactions between the HOMO and LUMO densities and the dipolar solvent. As shown in Fig. 3, the acceptor fragments in **7** and **8** are different, as shown by the LUMO of these dyes. Accordingly, their responses to environmental variations are different, in agreement with the different contributions of the solvent acidity and polarizability to their transition energies, obtained from Eqs. (2) and (3).

#### 4. Conclusions

The solvatochromic trends of dyes **7–9** were different in protic and non-protic media. In the former, a blue shift resulted from increasing the acidity of the alcoholic solvent, a result which reflected the increasing strength of the hydrogen-bond formed between the solvent and the anionic nitrogen atom. In non-protic solvents  $\lambda_{\max}$  values for a given dye were generally larger than in alcoholic media with little consistent variation of the transition energies with the medium polarity.

The solvatochromism of these compounds was governed by the acidity and polarizability of the medium, according to a multiparametric regression analysis performed with all compounds. The nitro-derivative **8** responded differently from its analogs **7** and **9** to the dipolarity–polarizability of the solvent, an effect which was rationalized by a theoretical analysis of the internal charge-transfer transition of dyes **7** and **8**. Thus it was shown that the acceptor fragment in the two compounds was different, charge being transferred to the dinitrophenylazo group in the case of dye **7**, and to the nitro-substituted phenyl group in the case of **8**.

Dye **8** was found to be more solvated by DMSO than by MeOH in a study of preferential solvation in this binary mixture.

#### Acknowledgements

Support by Fondecyt project # 1070124 is gratefully acknowledged.

#### References

- [1] Trujillo A, Fuentealba M, Manzur C, Carrillo D, Hamon JR. *J Organomet Chem* 2003;681:150–7.
- [2] Serbutoviez C, Bosshard C, Knöpfle G, Wyss P, Prêtre P, Günter P, et al. *Chem Mater* 1995;7:1198–206.
- [3] Asiri AM, Fatani NA. *Dyes Pigments* 2007;72:217–22.
- [4] Bakir M, Hassan I, Johnson T, Brown O, Green O, Gyles C, et al. *J Mol Struct* 2004;688:213–22.
- [5] Peng O, Li M, Gao K, Cheng L. *Dyes Pigments* 1991;15:263–74.
- [6] Stoyanov S, Ijima T, Stoyanova T, Antonov L. *Dyes Pigments* 1995;27:237–47.
- [7] Fayed TA. *Chem Phys* 2006;324:631–8.
- [8] El-Sayed M, Müller H, Rheinwald G, Lang H, Spange S. *Chem Mater* 2003;15:746–54.
- [9] Chou SSP, Sun DJ, Lin HC, Yang PK. *Chem Commun* 1996;1045–6.
- [10] Effenberger F, Würthner F, Steybe F. *J Org Chem* 1995;60:2082–91.
- [11] Hartmann H, Eckert K, Schröder A. *Angew Chem Int Ed* 2000;39:556–8.
- [12] Furniss BS, Hannaford AJ, Smith PWG, Tatchell AR. *Vogel's textbook of practical organic chemistry*. 5th ed. Essex: Longman; 1989. p. 1034.
- [13] Zhang Z, Dong YW, Wang GW. *Chem Lett* 2003;32:966–7.
- [14] Rezende MC, Pizarro C, Millán D. *Química Nova* 2007;30:229–31.
- [15] Johnson GD. *J Am Chem Soc* 1953;75:2720–3.
- [16] Tolochko AF, Schevchuk MI, Dombrovskii AV. *Zh Org Khim (Russian J Org Chem)* 1972;8:2397–402.
- [17] Frisch MJ, Trucks GW, Schlegel HB, Scuseria GE, Robb MA, Cheeseman JR, et al. *Gaussian 03, Revision C.02*. Wallingford CT: Gaussian, Inc.; 2004.
- [18] Zerner MC. Semi empirical molecular orbital methods. In: Lipkowitz KB, Boyd DB, editors. *Reviews of computational chemistry*, vol. 2. New York: VCH; 1991. p. 313.
- [19] Becke AD. *J Chem Phys* 1993;98:5648.
- [20] Bauernschmitt R, Ahlrichs R. *Chem Phys Lett* 1996;256:454.
- [21] Casida ME, Jamorski C, Casida KC, Salahub DR. *J Chem Phys* 1998;108:4439.
- [22] Reichardt C. *Solvents and solvent effects in organic chemistry*. 3rd ed. Weinheim: Wiley-VCH; 2003. p. 418–24.
- [23] Rosés M, Ràfols C, Ortega J, Bosch E. *J Chem Soc Perkin Trans* 1995;2:1607–15.
- [24] Skwierzynski RD, Connors KA. *J Chem Soc Perkin Trans* 1994;2:467–72.
- [25] Dreuw A, Head-Gordon M. *Chem Rev* 2005;105:4009–37.
- [26] Catalán J, Díaz C. *Liebigs Ann/Recueil* 1997;1941–9.
- [27] Catalán J, López V, Pérez P, Martín-Villamil R, Rodríguez JG. *Liebigs Ann* 1995;241–52.